Heating Mode Transition Induced by a Magnetic Field in a Capacitive rf Discharge

M. M. Turner, D. A. W. Hutchinson, R. A. Doyle, and M. B. Hopkins
School of Physical Sciences, Dublin City University, Dublin, Ireland
(Received 30 November 1995; revised manuscript received 6 February 1996)

We show that a recently proposed pressure model of collisionless heating in capacitive rf discharges predicts that a small magnetic field (~10 G) applied transverse to the electric field will induce a heating mode transition from a pressure-heating dominated state to an Ohmic-heating dominated state. This prediction is confirmed by kinetic simulations and experiments.

PACS numbers: 52.50.Gj, 52.65.Rr

Under appropriate conditions a capacitive rf discharge can be excited in large part by a collisionless electron heating mechanism, long believed to be a stochastic interaction between the discharge electrons and the time-varying electric fields that are found in the plasma sheaths. The sheaths in a capacitive discharge present a potential barrier that is large compared to the typical energies of plasma electrons, so when an electron enters a sheath it is likely to be reflected back into the plasma. Since the sheath fields vary in time, the interaction between the electron and the sheath is usually not conservative and the electron can gain or lose energy. Under certain assumptions the energy change can be shown to be positive on the average [1–4]. This model of the electron-sheath interaction is appealing—indeed almost compelling. However, in [5] we brought it in question: We constructed a model plasma with periodic boundary conditions but otherwise analogous to a capacitive discharge plasma and we showed that collisionless heating persisted in the model system. We further showed that the collisionless heating could be associated with the compression and rarefaction of electrons flowing through the inhomogeneous plasma. This effect we described as pressure heating. These results show that the collisionless heating remains when the sheath fields are absent, and therefore that the stochastic heating model is at least incomplete. (Note that we here use the term "collisionless heating" to refer to the undoubted phenomenon, and "stochastic heating" and "pressure heating" to describe contending explanatory models.) In this Letter we extend this argument to show that the pressure heating model predicts a novel effect—the occurrence of a heating mode transition in the presence of a weak magnetic field. The pressure heating model implies that the collisionless heating component can be essentially removed by a transverse magnetic field of as little as 10 G. This is of interest in itself and because a generalization of the stochastic heating model predicts an *enhancement* of collisionless heating in the presence of a magnetic field [6]. We have explored this issue both experimentally and using kinetic simulations. The results are consistent with the pressure model predictions—we find no indications of enhanced collisionless heating when the magnetic field is applied. On the contrary, we find evidence of a collisionless to Ohmic heating mode transition analogous to the one that can be induced by increasing the discharge pressure [7].

The generalization of the pressure heating model of [5] to a magnetized discharge consists essentially of introducing the magnetic field into the force terms in the momentum and energy balance equations, and a magnetic-field dependent electron thermal conductivity κ_e into the energy balance equation such that

$$\kappa_e(0)/\kappa_e(\omega_c) = 1 + \omega_c^2/\nu_e^2, \tag{1}$$

where $\kappa_e(0) = k_B T_e/m_e\nu_e$, ν_e is the electron neutral collision frequency, T_e is the electron temperature, ω_c is the angular electron cyclotron frequency, and $\omega_{\rm rf}$ is the angular driving frequency. The analysis of [5] can be repeated for these generalized equations. We find the generalized result for the ratio of the time-averaged and space-integrated pressure heating and Ohmic heating to be [cf. Eq. (6) of [5]]

$$\frac{P_{\rm pressure}}{P_{\rm Ohmic}} = \frac{5}{16}\frac{L}{x_0}[(1 + \gamma^2\beta^2)\Gamma]^{-1}, \tag{2}$$

where L is the half-width of the discharge, x_0 is a parameter (defined exactly in [5]) characterizing the space dependence of the electron density and time-averaged electron temperature, $\beta = 3\omega_{\rm rf}x_0^2/8\bar{\kappa}_e(0)$, $\gamma = 1 + \omega_c^2/\bar{\nu}_e^2$, $\Gamma = 1 + \omega_c^2/(\omega_{\rm rf}^2 + \bar{\nu}_e^2)$, and the barred quantities are space and time averaged. Equation (2) shows that the ratio of pressure heating to Ohmic heating goes rapidly to zero when some threshold magnetic field is exceeded, since $P_{\rm pressure}/P_{\rm Ohmic} \sim \omega_c^{-6}$ for ω_c sufficiently large. The absolute magnitude of the pressure heating also diminishes as the magnetic field is increased. The stochastic heating model has also been generalized for the magnetized case in [6], with the result that

$$P_{\rm stochastic} = \frac{1}{2}m_e n_e \upsilon_{\rm th}|u_s|^2 \frac{\omega_c}{\pi(\nu_e^2 + \omega_{\rm rf}^2)}\left(\nu_e + \frac{\omega_c}{\pi}\right), \tag{3}$$

where u_s is the sheath edge velocity amplitude and $\upsilon_{\rm th}$ is the electron thermal speed, so that when ω_c is large $P_{\rm stochastic} \sim \omega_c^2$ and $P_{\rm stochastic}/P_{\rm Ohmic}$ is independent of the magnetic field, since in the cases we consider here the

 © 1996 The American Physical Society

variations of u_s and $v_{\rm th}$ are relatively unimportant. Although this expression is not valid for weak magnetic fields with $\omega_c \lesssim \omega_{\rm rf}, \nu_e$ we should expect to find enhanced stochastic heating when $\omega_c \gtrsim \omega_{\rm rf}, \nu_e$.

Our simulation is based on the particle in cell algorithm with Monte Carlo collisions (PIC-MCC) [8–10], as in [5]. The results we discuss here were obtained from a bounded simulation extended along the x axis with a uniform magnetic field applied in the z direction and no fields in the y direction. Collision frequencies appropriate for a discharge in argon gas at 10 mTorr were used in the Monte Carlo collision handler. The electrodes were assumed to absorb all incident particles, and the discharge was driven by a current source with an amplitude of 1 mA cm^{-2} at angular frequency $\omega_{\rm rf} = 2\pi \times 13.56$ MHz. We selected the numerical parameters to satisfy the usual stability and accuracy conditions for explicit PIC codes [8,10]. Figure 1 shows the time-averaged electron heating as a function of the applied magnetic field. It is clear that the bulk heating increases monotonically with the magnetic field while the heating in the sheath regions varies in a more complicated way. The heating in the sheath regions is not entirely collisionless; we need to separate the components due to different processes to obtain a clear picture. The total heating in this bounded system may be regarded as composed of the collisionless heating, Ohmic heating, and evaporation cooling associated with the escape of electrons to the walls. The Ohmic heating can be calculated using the Langevin conductivity while the cooling term can be estimated by noting that the majority of electrons that escape do so when a sheath is fully collapsed, or nearly so. At this time the potential between the bulk plasma and the wall is approximately the floating potential [11]. Hence we can separate the time-averaged and space-integrated power into the three parts denoted in Fig. 2, which shows that the collisionless heating component indeed diminishes monotonically as the magnetic field is increased. The absolute value of the ratio given by Eq. (2) is in only fair agreement with the simulation results; from the simulation we have $P_{\rm collisionless}/P_{\rm Ohmic} \sim 2$ in the absence of the magnetic field but when appropriate parameters are inserted into Eq. (2) we find $P_{\rm pressure}/P_{\rm Ohmic} \sim 1$. Given that the plasma density and temperature profiles assumed in the derivation of Eq. (2) are approximations limited in accuracy by the functional forms of $n_e(x)$ and $T_e(x)$ adopted in [5], this is reasonable agreement. The parametric variation with the magnetic field is in much better agreement as Fig. 3 indicates. The magnetic field induces a heating model transition analogous to the effect of increasing the pressure [7], and the analogy extends to the change in the character of the electron energy distribution function which has the well-known bi-Maxwellian form [7,12] when the B field is absent and changes to a Druyvestyn-like shape with a sharp increase in the effective temperature when the magnetic field is applied. This transformation of the electron energy distribution function can be seen in experiments [13]. It may seem surprising that there is no overt indication of the electron cyclotron resonance in these data, but the resonance appears in the electric field in the bulk plasma, shown in Fig. 4, which passes through a minimum at $\omega_c = \omega_{\rm rf}$. This feature is less clear in the analytic model results (also shown in Fig. 4), in which the electric field connected with the pressure effect masks the electron cyclotron resonance.

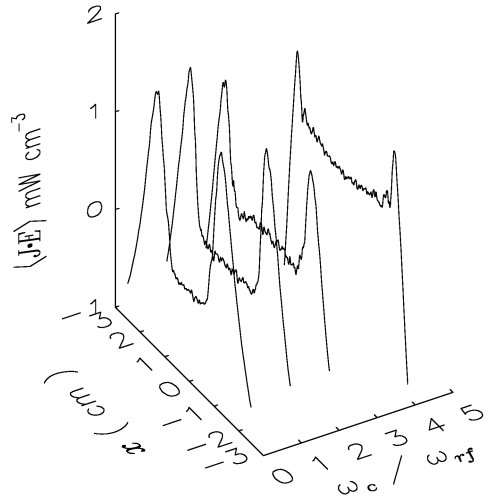

FIG. 1. Results from the PIC-MCC simulation described in the text. The time-averaged electron heating $\langle \mathbf{J} \cdot \mathbf{E} \rangle$ as a function of applied magnetic field expressed as the ratio of the cyclotron frequency ω_c to the driving frequency $\omega_{\rm rf}$.

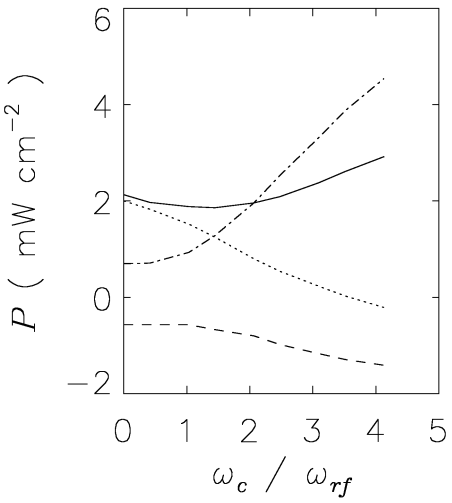

FIG. 2. The time-averaged and space-integrated power delivered to the electrons as a function of the applied magnetic field expressed as the ratio of the cyclotron frequency ω_c to the driving frequency $\omega_{\rm rf}$. The solid line shows the total power, the dashed line shows the evaporation cooling term $P_{\rm evaporation}$, the dotted line shows the collisionless heating $P_{\rm collisionless}$, and the dot-dashed line shows the Ohmic heating term $P_{\rm Ohmic}$. All the component terms are computed as described in the text; the total power is taken directly from the PIC-MCC simulation.

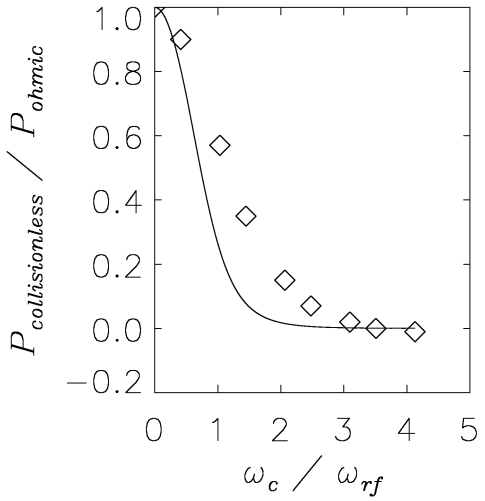

FIG. 3. The ratio of the collisionless heating $P_{\text{collisionless}}$ to the Ohmic heating P_{Ohmic} arbitrarily normalized at the origin. The solid line is the pressure-heating prediction from Eq. (2) and the symbols denote the ratio of the simulation results shown as $P_{\text{collisionless}}$ and P_{Ohmic} in Fig. 2.

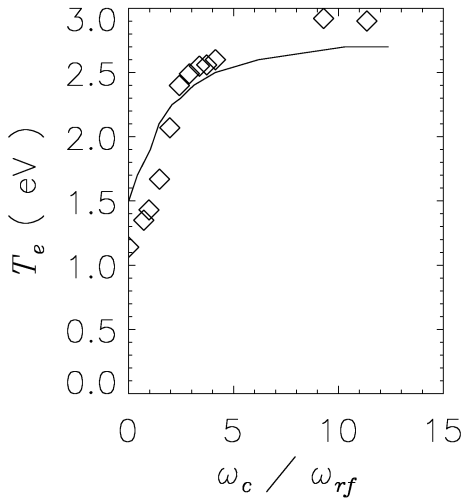

FIG. 5. Experimental measurements (symbols) of the effective electron temperature T_e at the midplane of the discharge compared with the results of PIC-MCC simulation (solid line), for the experimental conditions described in the text.

The experiments were performed on a capacitively coupled rf discharge formed in 10 mTorr of argon between a pair of plane stainless steel electrodes of approximately 10 cm radius and 7.5 cm separation. One electrode was grounded while the other was driven with a rf voltage at a frequency of 13.56 MHz. The voltage was adjusted during the experiments to maintain a constant current of 1 A. Both electrodes were enclosed in a stainless steel vacuum chamber. A continuously variable and approximately uniform magnetic field was applied to the discharge region using a pair of Tesla coils, the arrangement of which delivered magnetic fields of up to 20 G; larger fields were produced by applying permanent magnets to the outside of the vacuum chamber. While the magnetic field was varied the plasma was characterized using tuned Langmuir probes and a microwave interferometer [14]. Here we report only the most essential results; details have appeared elsewhere [13]. In Fig. 5 we show the effective electron temperature measured by the Langmuir probe, compared with the results of a PIC-MCC simulation with parameters appropriate to the experiment. There is evidently a sharp rise in the temperature produced by the magnetic field, with good agreement between simulation and experiment. Figure 6 shows the electron density measured by the Langmuir probe and by microwave interferometry. These data show a collapse in the electron density that the simulation does

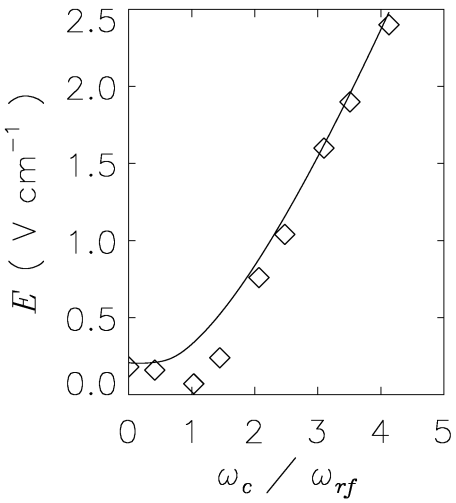

FIG. 4. The amplitude of the electric field at the discharge midplane, from pressure-heating theory (solid line) and the simulation (symbols).

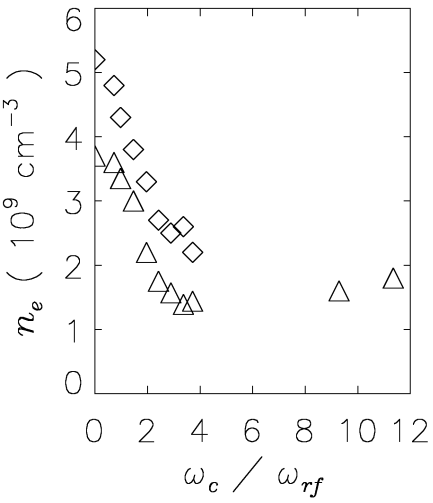

FIG. 6. Experimental measurements of the electron density at the discharge midplane using the Langmuir probe (triangles) and the microwave interferometer (diamonds), for the experimental conditions described in the text.

not predict adequately. We note that this problem occurs also in simulations of unmagnetized discharges when a heating mode transition threshold is crossed [12], and here magnetic confinement effects contribute and are exaggerated by the use of a one dimensional simulation. There is a striking parallel between these experimental results and those of [7], where the pressure induced heating mode transition was first reported. It seems inevitable that we should interpret our data as showing a heating mode transition also—the one predicted above by the pressure model of the collisionless heating mechanism. We have extended our computational and experimental investigations to magnetic fields substantially larger than those reported here (up to $\sim$100 G) and we have not found any evidence for collisionless heating scaling according to Eq. (3).

These results have a significance that goes further than the theory of magnetized capacitive discharges. Orthodox stochastic heating models applicable to unmagnetized discharges [1–4] locate the electron heating at the sheath edge and associate it with the large electric fields that occur in the sheath. Consequently, it is usually thought permissible to neglect the relatively weak electric fields in the plasma adjacent to the sheath, and nearly all non-self-consistent treatments do neglect these fields. Against this view, we showed in [5] that these presheath fields are responsible for the powerful collisionless heating process that we called pressure heating. This conclusion was somewhat presaged in [15,16]. The pressure heating mechanism was shown [5] to account for at least a large fraction of the collisionless heating that is observed in capacitive rf discharges. However, it remained as a possibility that there are two heating mechanisms, and that some of the collisionless heating could be described as stochastic. We believe that the results of the present Letter substantially reduce the remaining scope for this case. If there is any collisionless heating that is not pressure heating, we have shown that it has to scale in the presence of a magnetic field in a way consistent with Eq. (2) and this is not the scaling that is presently predicted for stochastic heating [6]. In spite of successes (e.g., the excellent agreement with experiments of [4]), the stochastic heating model is therefore in difficulty. We note in closing that the results in this Letter have another implication: We have shown that a capacitive rf discharge is measurably perturbed by a magnetic field less than an order of magnitude larger than the geomagnetic field. It is not difficult to inadvertently produce such a field. Evidently, care needs to be taken to ensure that this does not occur in precision experiments.

[1] V. A. Godyak, *Soviet Radio Frequency Discharge Research* (Delphic Associates, Inc., Falls Church, VA, 1986).
[2] M. A. Lieberman, IEEE Trans. Plasma Sci. **16**, 638 (1988).
[3] I. D. Kaganovich and L. D. Tsendin, IEEE Trans. Plasma Sci. **20**, 86 (1992).
[4] B. P. Wood, M. A. Lieberman, and A. J. Lichtenberg, IEEE Trans. Plasma Sci. **23**, 89 (1995).
[5] M. M. Turner, Phys. Rev. Lett. **75**, 1312 (1995).
[6] M. A. Lieberman, A. J. Lichtenberg, and S. E. Savas, IEEE Trans. Plasma Sci. **19**, 189 (1991).
[7] V. A. Godyak and R. B. Piejak, Phys. Rev. Lett. **65**, 996 (1990).
[8] C. K. Birdsall and A. B. Langdon, *Plasma Physics via Computer Simulation* (Adam Hilger, Bristol, 1991).
[9] C. K. Birdsall, IEEE Trans. Plasma Sci. **19**, 65 (1991).
[10] R. W. Hockney and J. W. Eastwood, *Computer Simulation Using Particles* (Adam Hilger, Bristol, 1988).
[11] D. Vender and R. W. Boswell, IEEE Trans. Plasma Sci. **18**, 725 (1990).
[12] V. Vahedi *et al.*, Plasma Sources Sci. Technol. **2**, 273 (1993).
[13] D. A. W. Hutchinson, M. M. Turner, R. A. Doyle, and M. B. Hopkins, IEEE Trans. Plasma Sci. **23**, 636 (1995).
[14] L. J. Overzet and M. B. Hopkins, J. Appl. Phys. **74**, 4323 (1993).
[15] M. Surendra and M. Dalvie, Phys. Rev. E **48**, 3914 (1993).
[16] M. Surendra and D. Vender, Appl. Phys. Lett. **65**, 153 (1994).